Reducing uncertainty in local climate projections

Saïd Qasmi (said.qasmi@meteo.fr)
Centre National de Recherches Météorologiques https://orcid.org/0000-0002-1825-3896
Aurélien Ribes
Centre National de Recherches Météorologiques https://orcid.org/0000-0001-5102-7885

Article

Keywords: climate change, climate projections, adaptation, temperature

Posted Date: May 4th, 2021

DOI: https://doi.org/10.21203/rs.3.rs-364943/v1

Reducing uncertainty in local climate projections

Saïd Qasmi*,[1] and Aurélien Ribes[1]

[1]CNRM, Université de Toulouse, Météo-France, CNRS, Toulouse, France

*Corresponding author: said_qasmi@meteo.fr

Abstract

Planning for adaptation to climate change requires accurate climate projections. Recent studies have shown that the uncertainty in global mean surface temperature projections can be considerably reduced by using historical observations. However, the transposition of these new results to the local scale is not yet available. Here we adapt an innovative statistical method that combines the latest generation of climate model simulations, global observations, and local observations to reduce uncertainty in local temperature projections. By taking advantage of the tight links between local and global temperature, we can derive the local implications of global constraints. The model uncertainty is reduced by 30% up to 50% at any location worldwide, allowing to substantially improve the quantification of risks associated with future climate change. A rigorous evaluation of these results within a perfect model framework indicates a robust skill, leading to a high confidence in our constrained climate projections.

Main

As the global mean temperature keeps rising and climate change intensifies, there is a growing demand for local scale monitoring of current and future climate change. Assessing and planning the adaptation to the expected unprecedented impacts of climate change on humans activities, ecosystems and the biosphere as a whole, require an accurate local information with well calibrated uncertainties. This need relates to estimates of warming to date and the future warming in response to set of scenarios of future greenhouse gas emissions.

There is now clear evidence that the recent increase of the average Earth's temperature is mostly due to human activities [1]. Concurrently, the anthropogenic influence is not detected everywhere at the local scale [2, 3]. Natural climate variability can blur the emergence of the anthropogenic signal for the next few years at high latitudes, while a significant warming is already reported in several tropical regions [4, 5]. Regarding climate projections, the IPCC concluded in its 5th assessment report (AR5) [6], that "Future [human-induced] warming trends cannot be predicted precisely, especially at local scales".

Since the AR5, a new generation of climate models [7] has been used to provide a range of projections in response to different socio-economic scenarios [8]. Based on this new dataset, various studies have recently shown that uncertainty in global mean warming can be considerably reduced by using the information provided by recent observed warming trends via so-called "constraint" methods [9, 10, 11, 12]. These studies consistently point towards a downward revision of the expected warming in

all emission scenarios [11, 9], with a decrease in model uncertainty of nearly 40% by 2100 [10], and even more at shorter lead times. This is an important result as, until then, observations have failed to provide clear evidence in reducing the range of climate projections [13].

The next challenge is to transpose these new findings on global warming to regional and local scales. At the regional scale, a few studies have adopted the partitioning from the Special Report on Managing the Risks of Extreme Events and Disasters to Advance Climate Change Adaptation [14] (SREX) and have attempted to narrow model uncertainty with sophisticated techniques with promising results [15, 16]. But the SREX regions are typically continental-wide, and do not provide relevant information for local adaptation. At the local scale, and to the best of our knowledge, no study has attempted to narrow the climate model uncertainty, except for specific and limited areas [17]. In particular, local climate projections are still solely based on a raw ensemble of available climate models in the IPCC AR5 [1].

Here we assess how much uncertainty in local temperature projections can be reduced. We first take advantage of the tight links that exist between local climate and global mean surface temperature (GMST) [18, 19]. Specifically, we describe the local implications of the recent advances in the reduction of the uncertainties in GMST projections. We then provide a set of local-scale temperature projections, which encapsulate another source of information: the observed local warming to date. If compared to the global mean temperature record, local observations are typically more affected by internal variability and measurement uncertainty. Yet, they still provide a useful source of information on both past and future trends, particularly

over some specific regions. We discuss how much these two types of observations (global and local) narrow uncertainty on future warming ranges. Such a reduction is expected to provide more accurate information that becomes critical for policy-makers in the local climate risk management [20], as well as for the climate science community.

The Kriging for Climate Change (KCC) method used by Ribes et al. [10], is one of the statistical techniques that have led to a major reduction of model uncertainty in GMST projections by combining observations and models. This Bayesian method involves first of all the definition of a prior distribution, which is here based on the temperature response simulated by the climate models, after filtering out internal variability as much as possible. This prior is subsequently conditioned by temperature observations over the historical period to derive a posterior probability distribution of the forced response, *i.e.*, a constrained temperature response, for both past and future periods. Compared to other constraint methods, in which observations are often summarised into one single variable, the KCC method is able to take the full observed time-series into account. Here, we further extend this technique in order to account for multiple time series, and potential dependencies between them (see Methods). When applied to the global surface air temperature (GSAT) time series simulated by the models from the Coupled Models Intercomparison Project phase 6 (CMIP6) [7] models and the Shared Socio-Economic Pathway (SSP) 5-8.5 scenario, the amplitude of the projected GSAT changes constrained by the observations is revised downwards by 0.5 °C by 2100, with a reduction in model uncertainty of nearly 40% [10]. Figure 1a offers an update of this result using GMST instead of

GSAT, with a downward revision of 0.6 °C. Difference with [10] are explained by the addition of several CMIP6 models, which affects the prior, and by the lower warming observed in GMST compared to GSAT [21, 22]. In the following, we consider the GMST metric to be consistent with the local observation dataset used (see Data).

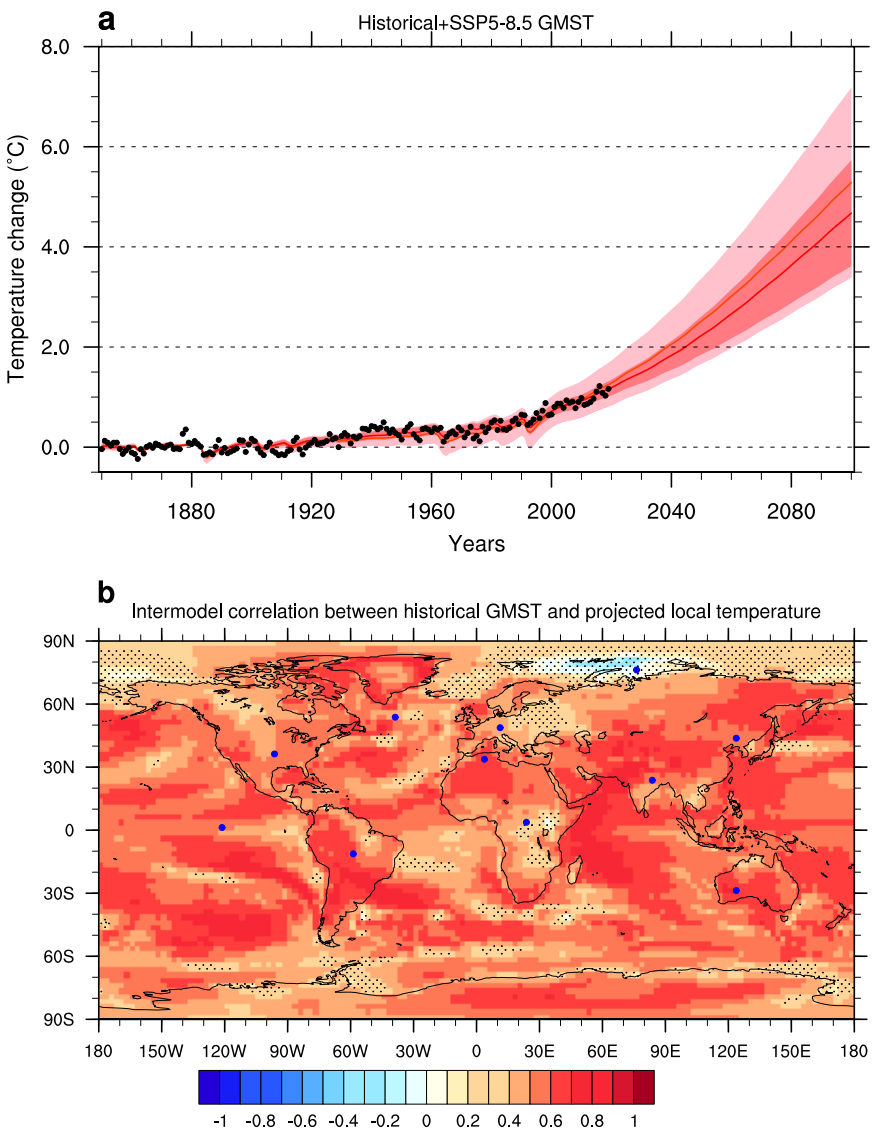

Fig. 1: **GMST time series and its correlation with local temperature.** (a) GMST annual observations (black points) are used to constrain concatenated historical and SSP5-8.5 scenario simulations of GMST. The unconstrained (pink) and constrained (red) ranges stand for the 5–95% confidence interval of the forced response as estimated from 28 CMIP6 models. The thick pink (red) line stands for the ensemble mean (best estimate). All values are anomalies with respect to the 1850–1900 period. (b) Intermodel correlation between simulated GMST trends over the 1850-2019 period and local temperature trends over the 2020-2100 period. Stippling indicates regions with non-significant correlation (p-value > 0.05 based on a two-sided Student's t-test).

Constrain local climate projections with global observations

Climate models exhibit a strong correlation between current GMST changes and future local warming over most regions of the globe (Figure 1b). To take such a relationship into account, we extend the KCC method to constrain local temperature projections. This is done by deriving the local warming conditional on the observed GMST record (hereafter the GMST-only case, see Methods and Supplementary Method 1). As an example, we consider the North American city of Dallas for which the simulated local temperature over the 2020-2100 period is significantly correlated with GMST (see the corresponding blue point in Figure 1b). Consistent with the constrained GMST, the constrained local temperature range indicates a decrease in uncertainty of about 30% over the 2081-2100 period (Figure 2a), and a downward revision of the best estimate of local warming by 0.4 °C compared to the unconstrained projections (hereafter the unconstrained case).

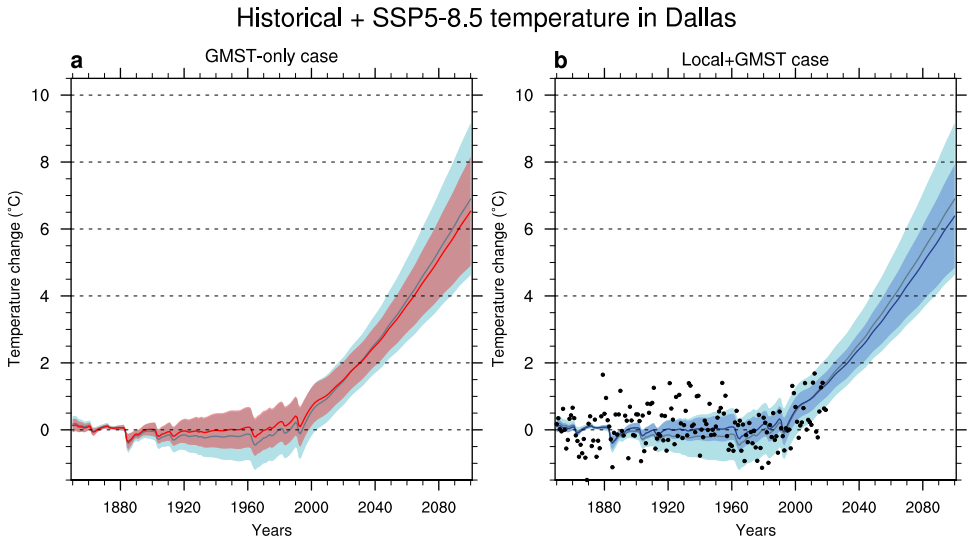

Fig. 2: **Observational constraints on historical and SSP5-8.5 local temperature changes in Dallas.** (a) Constrained local temperature for the grid point at [48.75 °N ; 11.25 °E] (see blue point in Figure 1b) in the GMST-only case. The constrained (unconstrained) 5–95% spread of the simulated response is in red (light blue), the red (grey) line stands for the best estimate (ensemble mean). (b) Constrained local temperature in the Local+GMST case. The constrained (unconstrained) 5–95% spread of the simulated response is in blue (light blue), its best estimate (ensemble mean) is in dark blue (grey). Black points are the observations. Unconstrained values are identical in a) and b). All values are anomalies with respect to the 1850–1900 period.

When the method is applied to any location worldwide, the results in the projected mean temperature and in model uncertainty depend on the level of correlation between the local temperature and GMST (Supplementary Figure 1cd and 1b). The reduction of uncertainty in local projections is the highest at the locations where the correlation with GMST is the strongest. For these locations, e.g. over several continental regions, the North Pacific and the Indian Ocean, a reduction of the ensemble spread of about 40% is obtained over the 2081-2100 period. In adition, the best es-

timate warming is revised downward from 0.5 °C to 1.5 °C. Conversely, for locations where the correlation is low, like in tropical Africa, the Barents Sea and the South Pacific gyre, the local temperature response is weakly constrained, with a reduction of the model uncertainty of 10% and a revision of the best estimate by 0.5 °C or less. These revised ranges lead to a warming pattern, at +2 °C of global warming, considerably different from the projections of the IPCC in its Special Report on Global Warming of 1.5 °C [23] (SR1.5) (Figure 3ad). For example, local temperatures over North America are expected to be 0.5 °warmer than in the unconstrained case under a global warming of 2 °C.

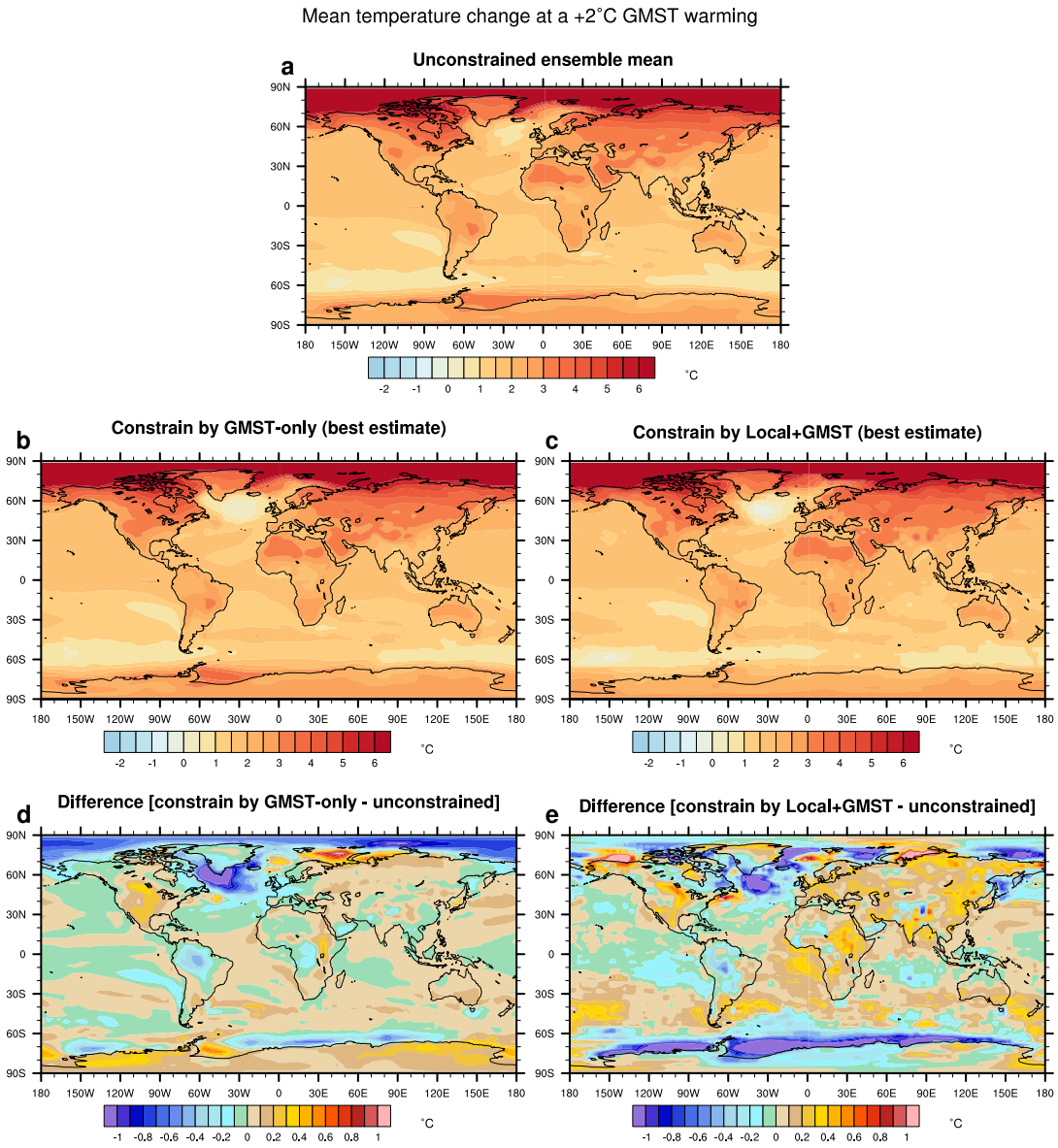

Fig. 3: **Warming pattern at +2 °C of GMST warming**. (a) Ensemble mean of the unconstrained local temperature changes. (b) Best estimate of the constrained local temperature changes in the GMST-only case. (c) Same as (b) but for the Local+GMST case. (d) Difference of local temperature changes between the GMST-only case (best estimate) and the unconstrained case (ensemble mean). (e) Difference of local temperature changes between the Local+GMST case (best estimate) and the unconstrained case (ensemble mean). All values in (a), (b) and (c) are anomalies with respect to the 1850-1900 period.

Added-value of local observations to the constraints

Beyond the useful information provided by the historical GMST time-series, one further very natural question involves the consistency between the expected local response (regardless whether observed GMST is accounted for) and local historical observations. Current and past warming is spatially heterogeneous, and some regions like the Arctic are warming faster than others [24] (Figure 3a). Evidence suggests that climate models have underestimated the Arctic temperature increase over the last few years [25]. This is in contradiction with the downward revision of the Beaufort Sea temperature change that is implied by the GMST-only constraint (Supplementary Figure 1c). Therefore, it is very attractive to account for both GMST and local observations to provide local projections consistent with all available observations. Using recent local observations could particularly affect short term projections (typically over the 2020-2030 period) and could provide a different picture of the constrained temperature ranges.

In order to make such a calculation, we derive a posterior of the expected local warming given local historical observations in addition to the GMST observations (hereafter the Local+GMST case, see Supplementary Method 1). Following the example of Dallas considered in Figure 2a, the constrained local temperature ranges become more consistent with local observations, particularly over the 2000-2019 period (Figure 2b). Compared to the GMST-only case, the added value of local observations in the reduction of model uncertainty is limited in this example, with a decrease of about 10% of the confidence range width compared to the GMST-only case. Two

reasons contribute to this limited impact. First, the local signal-to-noise ratio can be small. This may happen if local internal variability or measurement uncertainty is large (i.e., local observations provide little insight on the externally-forced response). Second, the global and local responses can be highly correlated with each other, so that they partly provide the same information, leading to a limited impact of local observations on uncertainty ranges. In both cases, the model uncertainty will be only marginally reduced by local historical data (Supplementary Method 1).

The application of the Local+GMST constraint to all grid points worldwide results in a global mean projected warming which is about the same as the GMST-only case (Supplementary Figure 1e), but with regional differences. On the one hand, for several regions over the Arctic, especially the Beaufort and Barents Seas, the warming is revised upwards compared to the unconstrained case, making the projections more consistent with recent observations, and implying a much higher warming than predicted in the GMST-only case. On the other hand, a downward revision is slightly strengthened over Northern Central Asia, Eastern North America, the East Siberian Sea, and along the Antarctica Coast. The added value of local observations in the reduction of model uncertainty is the largest over these regions where the correlation in Figure 1 is low (Supplementary Figure 1f). Note that for both the GMST-only and the Local+GMST cases, the global mean of the constrained local ranges is very close to the constrained GMST ranges shown in Figure 1a (not shown). The addition of local information can also clearly modify the warming pattern at +2 °C of global warming (Figure 3ce). For example, while a downward revision of the temperature change of -0.2 °C is obtained over Europe in the GMST-only case, an

upward revision of 0.3 °C is obtained in the Local+GMST case. This change of sign is widespread over Eurasia. In the context of an urgent need of adaptation to the threat of climate change, our constrained warming pattern provides a revised and a more relevant information for local adaptation planning.

Evaluation of the constrained projections

The robustness of these promising results is quantified within a so-called perfect model framework, using a leave-one-out cross validation technique. Each member of each model is considered as pseudo-observations over the 1850-2019 period. These are subsequently used to constrain the temperature projections, using all other models as a prior (Supplementary Method 2). The constrained temperature range is then compared to the true warming simulated by the model from which pseudo-observations were taken. As making this evaluation for all the grid points is computationally expensive, it has only been made at a few locations, considered as representative of the diversity of the worldwide climate (blue points in Figure 1b). As for the real observations, the method is applied for both the GMST-only and Local+GMST cases. The continuous ranked probability skill score (CRPSS) [26] is used to measure the accuracy of the method, taking the unconstrained projections as a baseline. This score is often used to assess the quality of an ensemble forecast, and measures the relative error between the predicted distribution and a given reference (Supplementary Method 2). A positive CRPSS indicates a better skill and a reduction of the error.

The median of the CRPSS distribution (based on all pseudo-observations) is positive for all selected points but the Arctic in the GMST-only case (where it comes close to 0, Figure 4). Depending on the region, the skill of the median is improved by 10% to 40% over the 2081-2100 period. In the Local+GMST case, the skill of the median is also positive for all regions, and lies between 10% and 50 % relative to the unconstrained case. The comparison between the Local+GMST and the GMST-only constraints shows that the skill of the median is positive for 8 out of 11 regions, and is slightly negative for only three regions (Mediterranean, Australia and Pacific). This suggests that there is often an added value in considering the constrained ranges derived from the Local+GMST case relative to the GMST-only case. A third case for which we only use local observations (Local-only case, Supplementary Figure 2) to constrain projections indicates lower scores than in the GMST-only and Local+GMST cases (Supplementary Figure 3), and confirms that using the combination of global and local observations enhances the accuracy of the method. The rare cases where the CRPSS is negative are attributed to the strong low-frequency internal variability in few models whose realism is debatable [27, 28] (Supplementary Method 2). A second evaluation criterion of the method based on coverage probabilities leads to similar conclusions (Supplementary Method 2). For these reasons, we retain the results from the Local+GMST case to assess the constrained local projections. This evaluation suggests that the constrained ranges are reliable, and that relying on unconstrained projections to assess local climate projections is no longer the best approach.

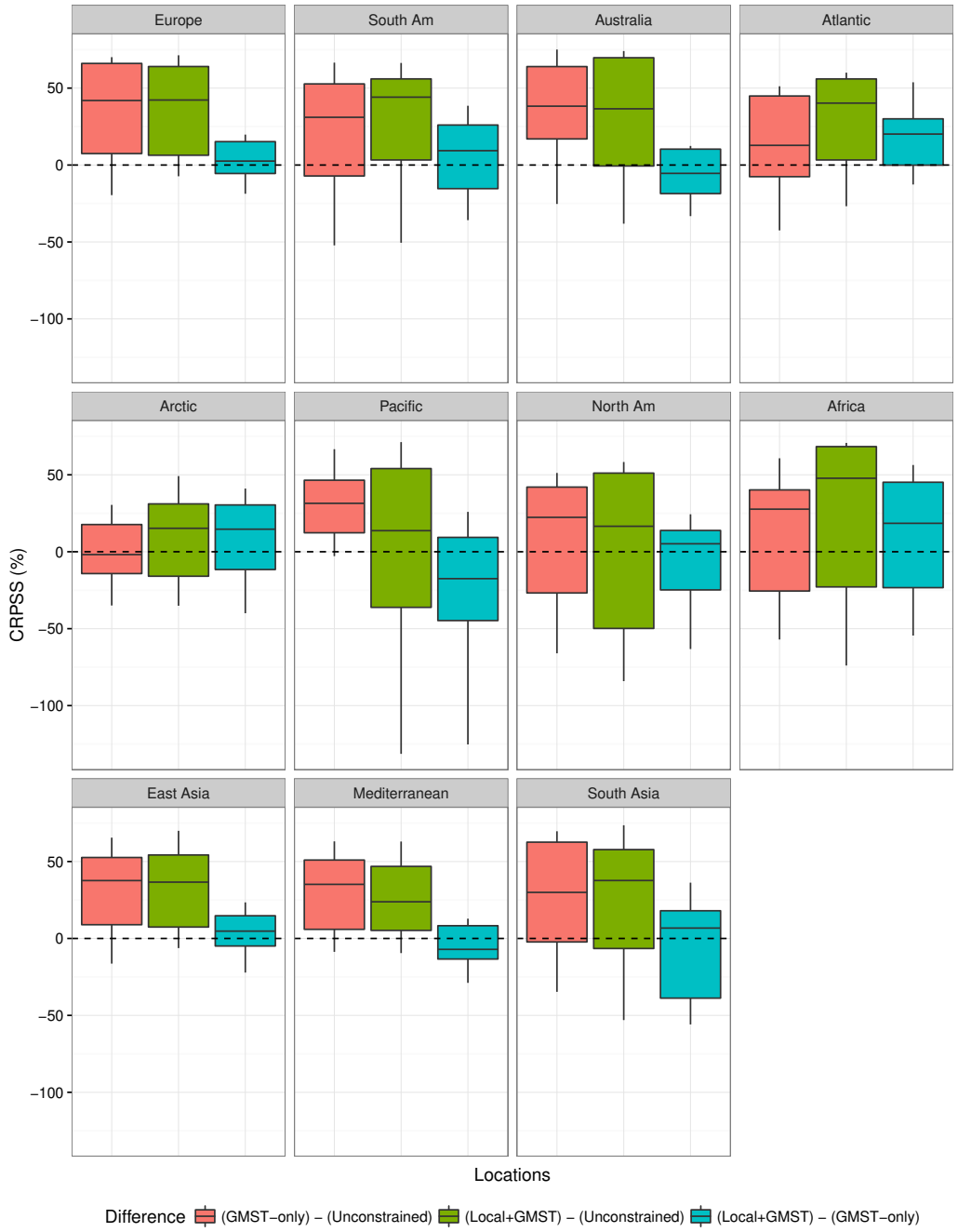

Fig. 4: **CRPSS for the constrained temperature projections over the 2081-2100 period within the perfect model framework.** Red (green) boxplots (one for each location, see blue points in Fig. 1b) indicate the CRPSS distributions in the GMST-only (Local+GMST) case compared to the unconstrained case. Blue boxplots indicate the added value from the local observations and stand for the CRPSS distributions in the Local+GMST case compared to the GMST-only case. The top (bottom) of the box represents the 25th (75th) percentile of the distribution and the upper (lower) whisker represents the 10th (90th) percentile. A CRPSS of 0 (dashed line) indicates the absence of added value of the method.

Implications for local pathways in a 2 °C warmer world

We have shown, using a statistical method combining the entire temperature observation records with model simulations, that uncertainty in local temperature projections can be substantially narrowed. Local projections constrained by both global and local observations exhibit a reduction of the uncertainty of 40% in average by 2100. This demonstrates the benefits of merging model simulations with observations to provide the best picture of future climate change. Figure 5 offers a complementary perspective to the IPCC SR1.5 [23] conclusions that were solely based on raw (unconstrained) projections. For each location, a temporal evolution from 1850 to 2100 of the constrained temperature and its uncertainty can be derived, with revised projections for the near and the long term time scales. This provides a considerable revision of the local exposure to the consequences of the on-going climate change [29]. An online tool that implements the method and illustrates the constrained temperature ranges for every point over a horizontal grid of 2.5 degree resolution is available via the following demonstrator: `https://saidqasmi.shinyapps.io/KCC-shinyapp/`.

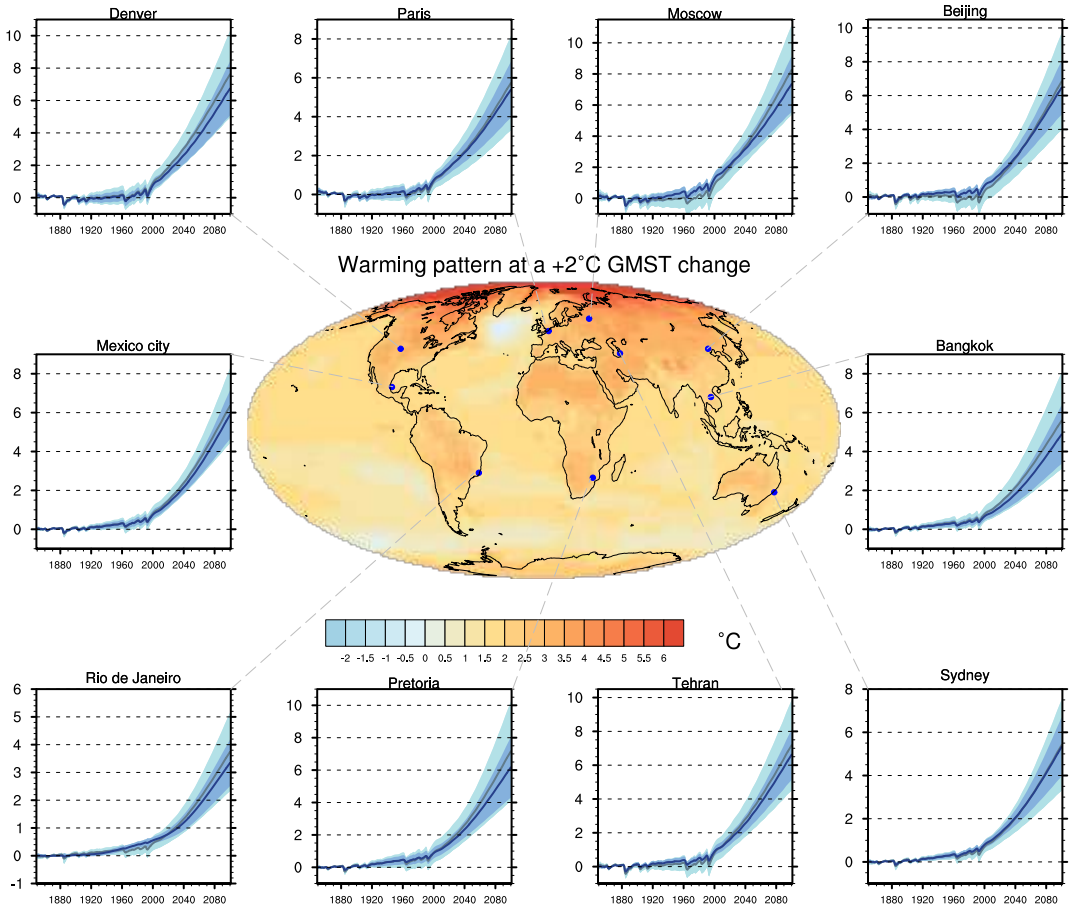

Fig. 5: **Mean temperature change at a +2 °C GMST warming**. Best estimate of the constrained local temperature changes in the Local+GMST case. Similarly to Figure 2b, the constrained and unconstrained temperature ranges are shown for several world capitals cities over the 1850-2100 period. All values are anomalies with respect to the 1850–1900 period.

Promising prospects exist to improve the method. CMIP5 [30] and CMIP6 [7] sample model uncertainty in a probabilistic way by using all climate models as an "ensemble of opportunities" [31, 32]. This approach, in which our study fits, has several limitations that can bias the estimation of climate uncertainty [33]. One of them

is that each model output is considered as independent and contributes equally to the multi-model ensemble. This "model democracy" paradigm has been largely used to summarise projection information in IPCC assessment reports [6], even though it can be criticised [34]. Therefore, using a subset of models qualified as independent a priori, or weighting the models in this way [35, 36], before applying the observational constraint, may provide even more reliable results.

Our results demonstrate that available observations already offer valuable information to sharpen climate projections. As the climate system will continue to change over the next decades, observations will further constrain the local and the global responses to the increasing greenhouse effect. Therefore, it is critical to account for this new source of information and to regularly bridge the gap between monitoring recent changes and predicting future changes. This is particularly important as the spread among global climate models has not decreased over the last CMIP generations. With our new projection ranges, the storyline approach [37, 38, 39], which is increasingly adopted in the climate risk management, could be refined. Generalising the method to other variables of high societal impacts, e.g. extreme precipitation, droughts, snow cover, some of which are also tightly related to GMST changes, would also be very relevant. In this way the climate science community could take a step forward towards a more accurate assessment of past and future human-induced climate change.

Methods

Observational dataset and models

The temperature observations are from the Cowtan and Way [40] dataset (hereafter CW) which complements the HadCRUT4 [41] data by filling in the missing data over the 1850-2019 period. The temperature field comes from a blending of near-surface temperature and sea surface temperature using land sea mask and sea ice concentration. The measurement uncertainty of the CW dataset is estimated from a set of 100 equiprobable realisations. Most of the other observational products are included in the temperature range estimated by this set, which confirms our choice to consider the CW dataset as a reference.

CMIP6 models are selected according to the availability of the following data: at least 200 years of pre-industrial control simulation; at least one member of a historical simulation and one member of a projection simulation for the SSP5-8.5 scenario. In order to constrain the simulated temperatures at a grid point scale in a consistent way, a blended temperature field T_{blend} is computed in each CMIP6 model based on the formulation of Cowtan et al. [21]:

$$w_{\mathrm{air}} = (1 - f_{\mathrm{ocean}}) + f_{\mathrm{ocean}} f_{\mathrm{ice}} \tag{1}$$

$$T_{\mathrm{blend}} = w_{\mathrm{air}} T_{\mathrm{air}} + (1 - w_{\mathrm{air}}) T_{\mathrm{ocean}} \tag{2}$$

where T_{air}, T_{ocean}, f_{ice}, and f_{ocean} are for each grid point near surface temperature, sea surface temperature, sea ice concentration and sea area fraction. The 28 models for which these variables are available and which satisfy the above criteria are listed in Supplementary Table 1.

Observations and models are interpolated on a common horizontal grid of 2.5 degree resolution before calculating blended temperatures and applying the constraining method.

Statistical Method

The statistical method is based on the same one used by Ribes et al. [10], whose formulation and principle is similar to kriging, which is a method originally developed to interpolate geophysical data based on prior covariances. In Ribes et al., this method is applied to the analysis of time series from climate simulations of CMIP5 and CMIP6 models, and is used for several purposes: (i) reducing model uncertainty on past and future global warming estimated by CMIP and ScenarioMIP [8] simulations, (ii) reducing uncertainty on warming attributed to several external forcings via DAMIP [42] models, (iii) complete or statistically reconstruct missing simulations from other physically relevant simulations (e.g. using the so-called 1%CO2 simulations, in which the CO2 concentration increases by 1% each year, to reconstruct DAMIP historical simulations in which GHGs follow their historical concentrations, while other forcings are kept constant). Here we apply this method of Kriging for Climate Change (KCC) to reduce the model uncertainty in the past and future temperature changes simulated by CMIP6 models at each grid

point. Note that a confusion can be made with techniques based on so-called emergent constraints methods [43, 44]. Emergent constraints would usually consider the sole observed global warming trend (a single scalar); e.g. over the 1980-2019 period, to constrain the simulated temperature changes in the future. The KCC method has several advantages compared to this approach. Instead of simply constraining a trend over a sub-period, it uses the entire observed time series of temperature, which avoids ignoring useful information. In addition, the method takes into account the model temporal pattern uncertainty and provides confidence ranges specifically for the forced response, while many other studies also include internal variability.

For each grid point, we define $\boldsymbol{y}^*_{\text{loc}}$ as the yearly time series of the real (and unknwown) temperature response to external forcings over the 1850-2100 period, and $\boldsymbol{y}_{\text{loc}}$ as the observed yearly temperature time series over the 1850-2019 period. Similarly, we define $\boldsymbol{y}^*_{\text{glo}}$ and $\boldsymbol{y}_{\text{glo}}$ as the simulated and observed global mean near-surface temperature (GMST) time series, respectively, constituting the following $\boldsymbol{y}^*$ and $\boldsymbol{y}$ vectors:

$$\boldsymbol{y}^* = \begin{pmatrix} \boldsymbol{y}^*_{\text{loc}} \\ \boldsymbol{y}^*_{\text{glo}} \end{pmatrix}, \qquad \boldsymbol{y} = \begin{pmatrix} \boldsymbol{y}_{\text{loc}} \\ \boldsymbol{y}_{\text{glo}} \end{pmatrix} \tag{3}$$

Assuming that the observed temperature variability can be decomposed as the sum of a term of forced variability and a term including both internal variability and measurement errors, $\boldsymbol{y}$ take the following form:

$$\boldsymbol{y} = \boldsymbol{y}^* + \epsilon \tag{4}$$

where ϵ corresponds to the term of measurement errors and internal variability. Further assuming that models are indistinguishable from the truth, *i.e.* that observations and models are exchangeable, observations $\boldsymbol{y}$ can be rewritten:

$$\boldsymbol{y} = \boldsymbol{H}\boldsymbol{x} + \epsilon \tag{5}$$

where $\boldsymbol{x}$ is the yearly time series over the 1850-2100 period of the temperature response to external forcings estimated in CMIP6 models. $\boldsymbol{H}$ is an observation operator, which basically extracts the part of $\boldsymbol{x}$ that is observed in $\boldsymbol{y}$, *i.e.* the forced response from 1850 to 2019, and whose form depends on the type of the applied constraint (using only GMST or both GMST and local observations) .

The analyses are conducted within a Bayesian framework, allowing us to consider a multimodel ensemble of $\boldsymbol{x}$, from which a prior of $\boldsymbol{x}$, noted $\Pi(\boldsymbol{x})$, is derived. Assuming that $\Pi(\boldsymbol{x})$ and ϵ follow normal distributions allows to apply the Gaussian conditioning theorem, which strictly corresponds to the kriging interpolation, to derive the posterior $p(\boldsymbol{x}|\boldsymbol{y})$, *i.e.* the so-called "constrained" distribution by observations.

Full technical details on the calculation of $\Pi(\boldsymbol{x})$, $\boldsymbol{H}$ and $p(\boldsymbol{x}|\boldsymbol{y})$ and on the represen-

tation of internal variability are provided in the Supplementary Method 1 section.

All required programs to run the method are available from: `https://gitlab.com/saidqasmi/KCC`.

Acknowledgements

This work was supported by the European Union's Horizon 2020 Research and Innovation Programme in the framework of the EUCP project (Grant Agreement 776613) and Météo-France. The authors thank Hervé Douville for fruitful discussions about this work. The authors thank the climate modeling groups involved in CMIP6 exercises for producing and making available their simulations. The authors thank Kevin Cowtan for providing the blended temperature data, and the ETH Zurich for providing CMIP6 data through their cmip6-ng interface (`http://dx.doi.org/10.5281/zenodo.3734128`). The analyses and figures were produced with the R software (`https://www.R-project.org/`) and the NCAR Command Language Software (`http://dx.doi.org/10.5065/D6WD3XH5`).

Author information

S.Q. and A.R. contributed to the design of the study, the interpretation of the results and the writing of the manuscript. S.Q. processed the data and produced the figures.

Competing interests

The authors declare no competing interests.

References

[1] Bindoff, N. L. *et al.* Chapter 10 - Detection and attribution of climate change: From global to regional. In *Climate Change 2013: The Physical Science Basis. IPCC Working Group I Contribution to AR5* (Cambridge University Press, Cambridge, 2013). URL `http://pure.iiasa.ac.at/id/eprint/10552/`.

[2] Hawkins, E. & Sutton, R. Time of emergence of climate signals. *Geophysical Research Letters* **39** (2012). URL `https://agupubs.onlinelibrary.wiley.com/doi/abs/10.1029/2011GL050087`. _eprint: https://agupubs.onlinelibrary.wiley.com/doi/pdf/10.1029/2011GL050087.

[3] Hawkins, E. *et al.* Observed Emergence of the Climate Change Signal: From the Familiar to the Unknown. *Geophysical Research Letters* **47**, e2019GL086259 (2020). URL `http://agupubs.onlinelibrary.wiley.com/doi/abs/10.1029/2019GL086259`. _eprint: https://onlinelibrary.wiley.com/doi/pdf/10.1029/2019GL086259.

[4] Deser, C., Knutti, R., Solomon, S. & Phillips, A. S. Communication of the role of natural variability in future North American climate. *Nature Climate Change* **2**, 775–779 (2012). URL `http://www.nature.com/articles/nclimate1562`. Number: 11 Publisher: Nature Publishing Group.

[5] Mahlstein, I., Knutti, R., Solomon, S. & Portmann, R. W. Early onset of significant local warming in low latitude countries. *Environmental Research Letters* **6**, 034009 (2011). URL https://doi.org/10.1088/1748-9326/6/3/034009. Publisher: IOP Publishing.

[6] Collins, M. *et al.* Chapter 12 - Long-term climate change: Projections, commitments and irreversibility. In IPCC (ed.) *Climate Change 2013: The Physical Science Basis. IPCC Working Group I Contribution to AR5* (Cambridge University Press, Cambridge, 2013). URL http://pure.iiasa.ac.at/id/eprint/10551/.

[7] Eyring, V. *et al.* Overview of the Coupled Model Intercomparison Project Phase 6 (CMIP6) experimental design and organization. *Geoscientific Model Development* **9**, 1937–1958 (2016). URL https://www.geosci-model-dev.net/9/1937/2016/.

[8] O'Neill, B. C. *et al.* The Scenario Model Intercomparison Project (ScenarioMIP) for CMIP6. *Geoscientific Model Development* **9**, 3461–3482 (2016). URL https://gmd.copernicus.org/articles/9/3461/2016/. Publisher: Copernicus GmbH.

[9] Tokarska, K. B. *et al.* Past warming trend constrains future warming in CMIP6 models. *Science Advances* **6**, eaaz9549 (2020). URL https://advances.sciencemag.org/content/6/12/eaaz9549. Publisher: American Association for the Advancement of Science Section: Research Article.

[10] Ribes, A., Qasmi, S. & Gillett, N. P. Making climate projections conditional

on historical observations. *Science Advances* **7**, eabc0671 (2021). URL https://advances.sciencemag.org/content/7/4/eabc0671. Publisher: American Association for the Advancement of Science Section: Research Article.

[11] Brunner, L. *et al.* Reduced global warming from CMIP6 projections when weighting models by performance and independence. *Earth System Dynamics* **11**, 995–1012 (2020). URL https://esd.copernicus.org/articles/11/995/2020/. Publisher: Copernicus GmbH.

[12] Nijsse, F. J. M. M., Cox, P. M. & Williamson, M. S. Emergent constraints on transient climate response (TCR) and equilibrium climate sensitivity (ECS) from historical warming in CMIP5 and CMIP6 models. *Earth System Dynamics* **11**, 737–750 (2020). URL https://esd.copernicus.org/articles/11/737/2020/. Publisher: Copernicus GmbH.

[13] Schlund, M., Lauer, A., Gentine, P., Sherwood, S. C. & Eyring, V. Emergent constraints on equilibrium climate sensitivity in CMIP5: do they hold for CMIP6? *Earth System Dynamics* **11**, 1233–1258 (2020). URL https://esd.copernicus.org/articles/11/1233/2020/. Publisher: Copernicus GmbH.

[14] Field, C. B., Barros, V. & Dokken, D. J. *Managing the risks of extreme events and disasters to advance climate change adaption: special report of the Intergovernmental Panel on Climate Change* (Cambridge University Press, New York, NY, 2012). OCLC: ocn796030880.

[15] Brunner, L. *et al.* Comparing Methods to Constrain Future European Climate Projections Using a Consistent Framework. *Journal of Climate* **33**, 8671–

8692 (2020). URL https://journals.ametsoc.org/jcli/article/33/20/8671/348736/Comparing-Methods-to-Constrain-Future-European. Publisher: American Meteorological Society.

[16] Brunner, L., Lorenz, R., Zumwald, M. & Knutti, R. Quantifying uncertainty in European climate projections using combined performance-independence weighting. *Environmental Research Letters* **14**, 124010 (2019). URL https://doi.org/10.1088%2F1748-9326%2Fab492f. Publisher: IOP Publishing.

[17] Borodina, A., Fischer, E. M. & Knutti, R. Emergent Constraints in Climate Projections: A Case Study of Changes in High-Latitude Temperature Variability. *Journal of Climate* **30**, 3655–3670 (2017). URL https://journals.ametsoc.org/view/journals/clim/30/10/jcli-d-16-0662.1.xml. Publisher: American Meteorological Society Section: Journal of Climate.

[18] Sutton, R., Suckling, E. & Hawkins, E. What does global mean temperature tell us about local climate? *Philosophical Transactions of the Royal Society A: Mathematical, Physical and Engineering Sciences* **373**, 20140426 (2015). URL https://royalsocietypublishing.org/doi/10.1098/rsta.2014.0426. Publisher: Royal Society.

[19] Tebaldi, C. & Arblaster, J. M. Pattern scaling: Its strengths and limitations, and an update on the latest model simulations. *Climatic Change* **122**, 459–471 (2014). URL https://doi.org/10.1007/s10584-013-1032-9.

[20] Viner, D. *et al.* Understanding the dynamic nature of risk in climate change assessments—A new starting point for discussion. *At-*

mospheric Science Letters **21**, e958 (2020). URL https://rmets.onlinelibrary.wiley.com/doi/abs/10.1002/asl.958. _eprint: https://rmets.onlinelibrary.wiley.com/doi/pdf/10.1002/asl.958.

[21] Cowtan, K. *et al.* Robust comparison of climate models with observations using blended land air and ocean sea surface temperatures. *Geophysical Research Letters* **42**, 6526–6534 (2015). URL https://agupubs.onlinelibrary.wiley.com/doi/abs/10.1002/2015GL064888. _eprint: https://agupubs.onlinelibrary.wiley.com/doi/pdf/10.1002/2015GL064888.

[22] Richardson, M., Cowtan, K. & Millar, R. J. Global temperature definition affects achievement of long-term climate goals. *Environmental Research Letters* **13**, 054004 (2018). URL https://iopscience.iop.org/article/10.1088/1748-9326/aab305.

[23] Hoegh-Guldberg, O. *et al.* Impacts of 1.5°C global warming on natural and human systems. In *Global Warming of 1.5°C* (IPCC, 2018).

[24] Screen, J. A. & Simmonds, I. The central role of diminishing sea ice in recent Arctic temperature amplification. *Nature* **464**, 1334–1337 (2010). URL https://www.nature.com/articles/nature09051. Number: 7293 Publisher: Nature Publishing Group.

[25] Jansen, E. *et al.* Past perspectives on the present era of abrupt Arctic climate change. *Nature Climate Change* **10**, 714–721 (2020). URL http://www.nature.com/articles/s41558-020-0860-7. Number: 8 Publisher: Nature Publishing Group.

[26] Gneiting, T., Raftery, A. E., Westveld, A. H. & Goldman, T. Calibrated Probabilistic Forecasting Using Ensemble Model Output Statistics and Minimum CRPS Estimation. *Monthly Weather Review* **133**, 1098–1118 (2005). URL https://journals.ametsoc.org/mwr/article/133/5/1098/67504/Calibrated-Probabilistic-Forecasting-Using. Publisher: American Meteorological Society.

[27] Mann, M. E., Steinman, B. A., Brouillette, D. J. & Miller, S. K. Multidecadal climate oscillations during the past millennium driven by volcanic forcing. *Science* **371**, 1014–1019 (2021). URL https://science-sciencemag-org.insu.bib.cnrs.fr/content/371/6533/1014. Publisher: American Association for the Advancement of Science Section: Research Article.

[28] Haustein, K. *et al.* A Limited Role for Unforced Internal Variability in Twentieth-Century Warming. *Journal of Climate* **32**, 4893–4917 (2019). URL https://journals.ametsoc.org/view/journals/clim/32/16/jcli-d-18-0555.1.xml. Publisher: American Meteorological Society Section: Journal of Climate.

[29] Schleussner, C.-F. *et al.* Differential climate impacts for policy-relevant limits to global warming: the case of 1.5 °C and 2 °C. *Earth System Dynamics* **7**, 327–351 (2016). URL https://esd.copernicus.org/articles/7/327/2016/.

[30] Taylor, K. E., Stouffer, R. J. & Meehl, G. A. An Overview of CMIP5 and the Experiment Design. *Bulletin of the American Meteorological Society* **93**, 485–498 (2012). URL https://journals.ametsoc.org/doi/10.1175/

BAMS-D-11-00094.1.

[31] Tebaldi, C. & Knutti, R. The use of the multi-model ensemble in probabilistic climate projections. *Philosophical Transactions of the Royal Society A: Mathematical, Physical and Engineering Sciences* **365**, 2053–2075 (2007). URL https://royalsocietypublishing.org/doi/10.1098/rsta.2007.2076. Publisher: Royal Society.

[32] Sanderson, B. M., Knutti, R. & Caldwell, P. A Representative Democracy to Reduce Interdependency in a Multimodel Ensemble. *Journal of Climate* **28**, 5171–5194 (2015). URL https://journals.ametsoc.org/jcli/article/28/13/5171/106259/A-Representative-Democracy-to-Reduce. Publisher: American Meteorological Society.

[33] Eyring, V. *et al.* Taking climate model evaluation to the next level. *Nature Climate Change* **9**, 102–110 (2019). URL https://www.nature.com/articles/s41558-018-0355-y. Number: 2 Publisher: Nature Publishing Group.

[34] Sanderson, B. M. & Knutti, R. On the interpretation of constrained climate model ensembles. *Geophysical Research Letters* **39** (2012). URL https://agupubs.onlinelibrary.wiley.com/doi/abs/10.1029/2012GL052665. _eprint: https://agupubs.onlinelibrary.wiley.com/doi/pdf/10.1029/2012GL052665.

[35] Knutti, R. *et al.* A climate model projection weighting scheme accounting for performance and interdependence. *Geophysical Research Letters* **44**, 1909–1918 (2017). URL https://agupubs.

onlinelibrary.wiley.com/doi/abs/10.1002/2016GL072012. _eprint: https://agupubs.onlinelibrary.wiley.com/doi/pdf/10.1002/2016GL072012.

[36] Sanderson, B. M., Wehner, M. & Knutti, R. Skill and independence weighting for multi-model assessments. *Geoscientific Model Development* **10**, 2379–2395 (2017). URL https://gmd.copernicus.org/articles/10/2379/2017/. Publisher: Copernicus GmbH.

[37] Shepherd, T. G. Storyline approach to the construction of regional climate change information. *Proceedings. Mathematical, Physical, and Engineering Sciences* **475** (2019). URL https://www.ncbi.nlm.nih.gov/pmc/articles/PMC6545051/.

[38] Sutton, R. T. Climate Science Needs to Take Risk Assessment Much More Seriously. *Bulletin of the American Meteorological Society* **100**, 1637–1642 (2019). URL https://journals.ametsoc.org/view/journals/bams/100/9/bams-d-18-0280.1.xml. Publisher: American Meteorological Society Section: Bulletin of the American Meteorological Society.

[39] Zappa, G. Regional Climate Impacts of Future Changes in the Mid–Latitude Atmospheric Circulation: a Storyline View. *Current Climate Change Reports* **5**, 358–371 (2019). URL https://doi.org/10.1007/s40641-019-00146-7.

[40] Cowtan, K. & Way, R. G. Coverage bias in the HadCRUT4 temperature series and its impact on recent temperature trends. *Quarterly Journal of the Royal Meteorological Society* **140**, 1935–1944 (2014). URL https:

//rmets.onlinelibrary.wiley.com/doi/abs/10.1002/qj.2297. _eprint: https://rmets.onlinelibrary.wiley.com/doi/pdf/10.1002/qj.2297.

[41] Morice, C. P., Kennedy, J. J., Rayner, N. A. & Jones, P. D. Quantifying uncertainties in global and regional temperature change using an ensemble of observational estimates: The HadCRUT4 data set. *Journal of Geophysical Research: Atmospheres* **117** (2012). URL https://agupubs.onlinelibrary.wiley.com/doi/abs/10.1029/2011JD017187. _eprint: https://agupubs.onlinelibrary.wiley.com/doi/pdf/10.1029/2011JD017187.

[42] Gillett, N. P. *et al.* The Detection and Attribution Model Intercomparison Project (DAMIP v1.0) contribution to CMIP6. *Geoscientific Model Development* **9**, 3685–3697 (2016). URL https://gmd.copernicus.org/articles/9/3685/2016/. Publisher: Copernicus GmbH.

[43] Hall, A. & Qu, X. Using the current seasonal cycle to constrain snow albedo feedback in future climate change. *Geophysical Research Letters* **33** (2006). URL http://agupubs.onlinelibrary.wiley.com/doi/10.1029/2005GL025127.

[44] Hall, A., Cox, P., Huntingford, C. & Klein, S. Progressing emergent constraints on future climate change. *Nature Climate Change* **9**, 269–278 (2019). URL http://www.nature.com/articles/s41558-019-0436-6.

Figures

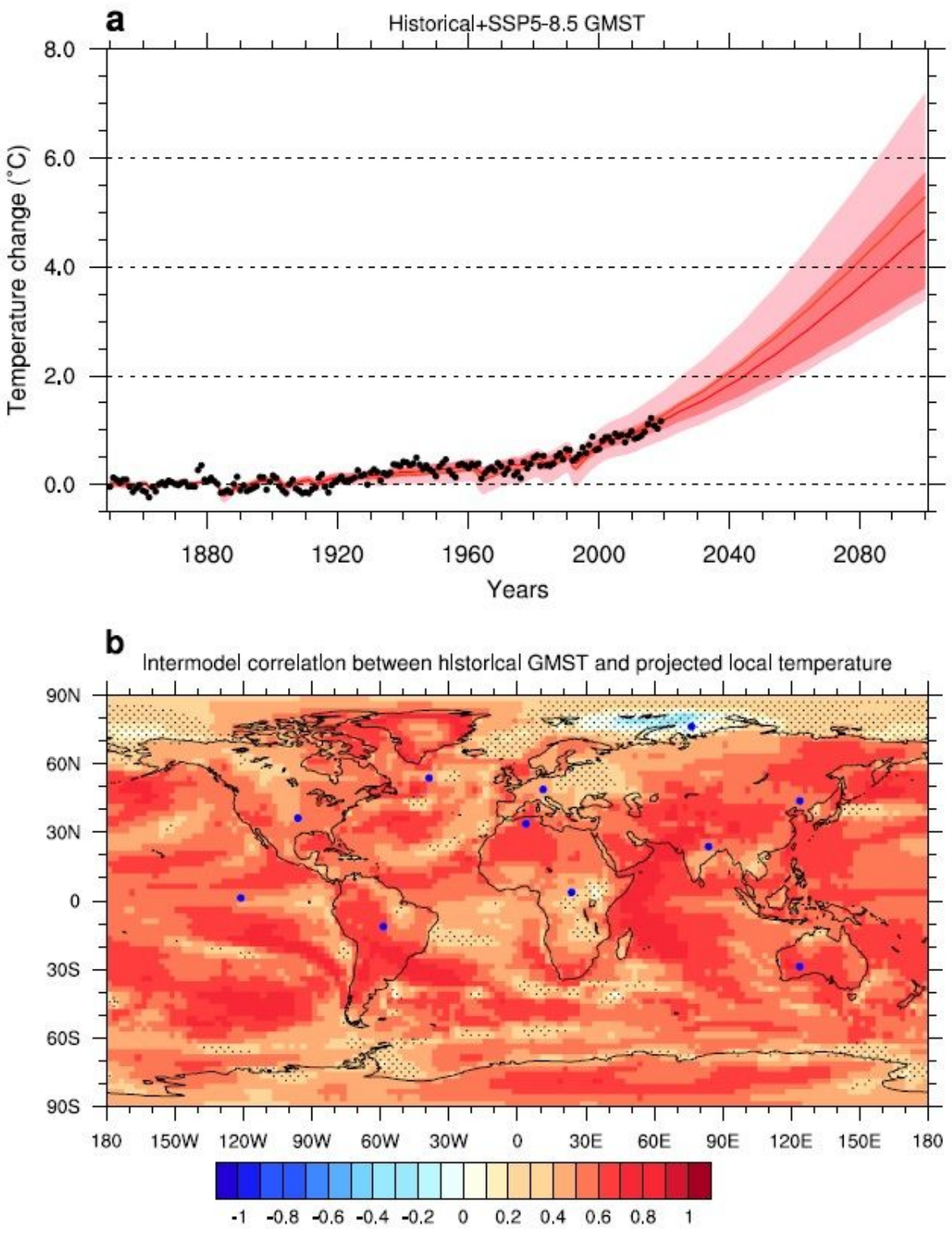

Figure 1

GMST time series and its correlation with local temperature. (a) GMST annual observations (black points) are used to constrain concatenated historical and SSP5-8.5 scenario simulations of GMST. The unconstrained (pink) and constrained (red) ranges stand for the 5{95% confidence interval of the forced

response as estimated from 28 CMIP6 models. The thick pink (red) line stands for the ensemble mean (best estimate). All values are anomalies with respect to the 1850{1900 period. (b) Intermodel correlation between simulated GMST trends over the 1850-2019 period and local temperature trends over the 2020-2100 period. Stippling indicates regions with non-significant correlation (p-value > 0:05 based on a two-sided Student's t-test). Note: The designations employed and the presentation of the material on this map do not imply the expression of any opinion whatsoever on the part of Research Square concerning the legal status of any country, territory, city or area or of its authorities, or concerning the delimitation of its frontiers or boundaries. This map has been provided by the authors.

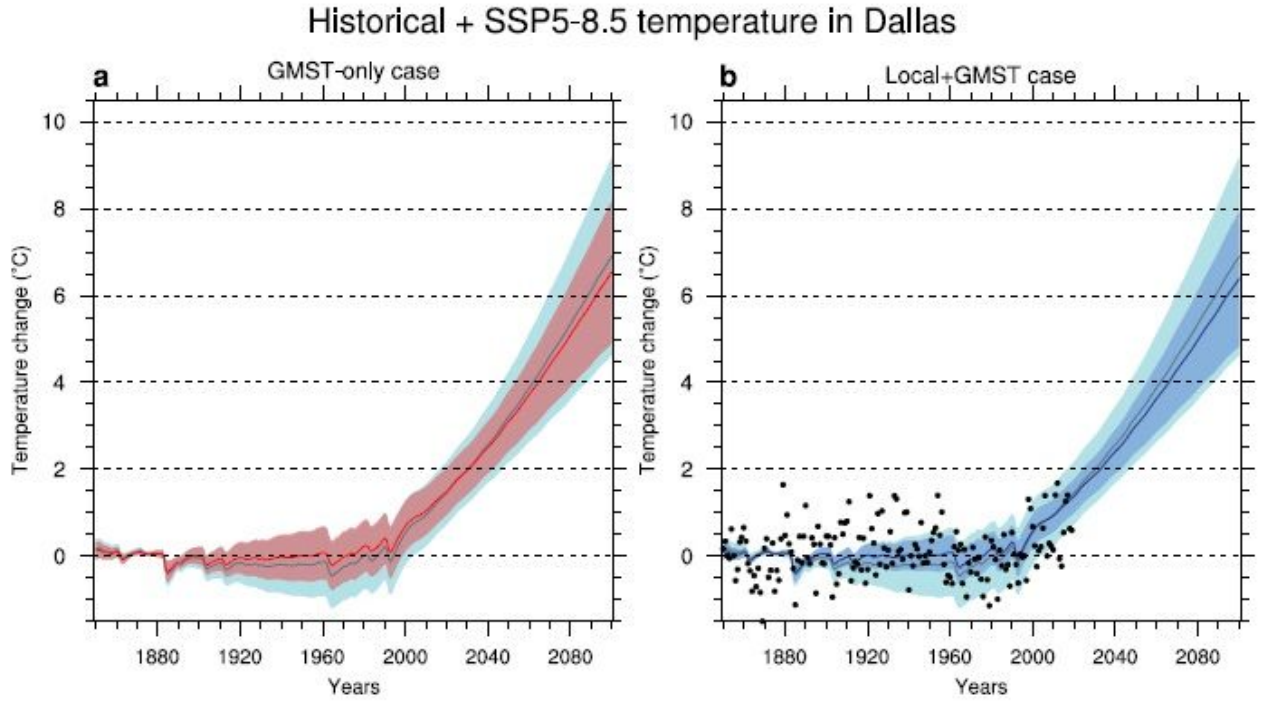

Figure 2

Observational constraints on historical and SSP5-8.5 local temperature changes in Dallas. (a) Constrained local temperature for the grid point at [48.75 oN ; 11.25 oE] (see blue point in Figure 1b) in the GMST-only case. The constrained (unconstrained) 5{95% spread of the simulated response is in red (light blue), the red (grey) line stands for the best estimate (ensemble mean). (b) Constrained local temperature in the Local+GMST case. The constrained (unconstrained) 5{95% spread of the simulated response is in blue (light blue), its best estimate (ensemble mean) is in dark blue (grey). Black points are the observations. Unconstrained values are identical in a) and b). All values are anomalies with respect to the 1850{1900 period.

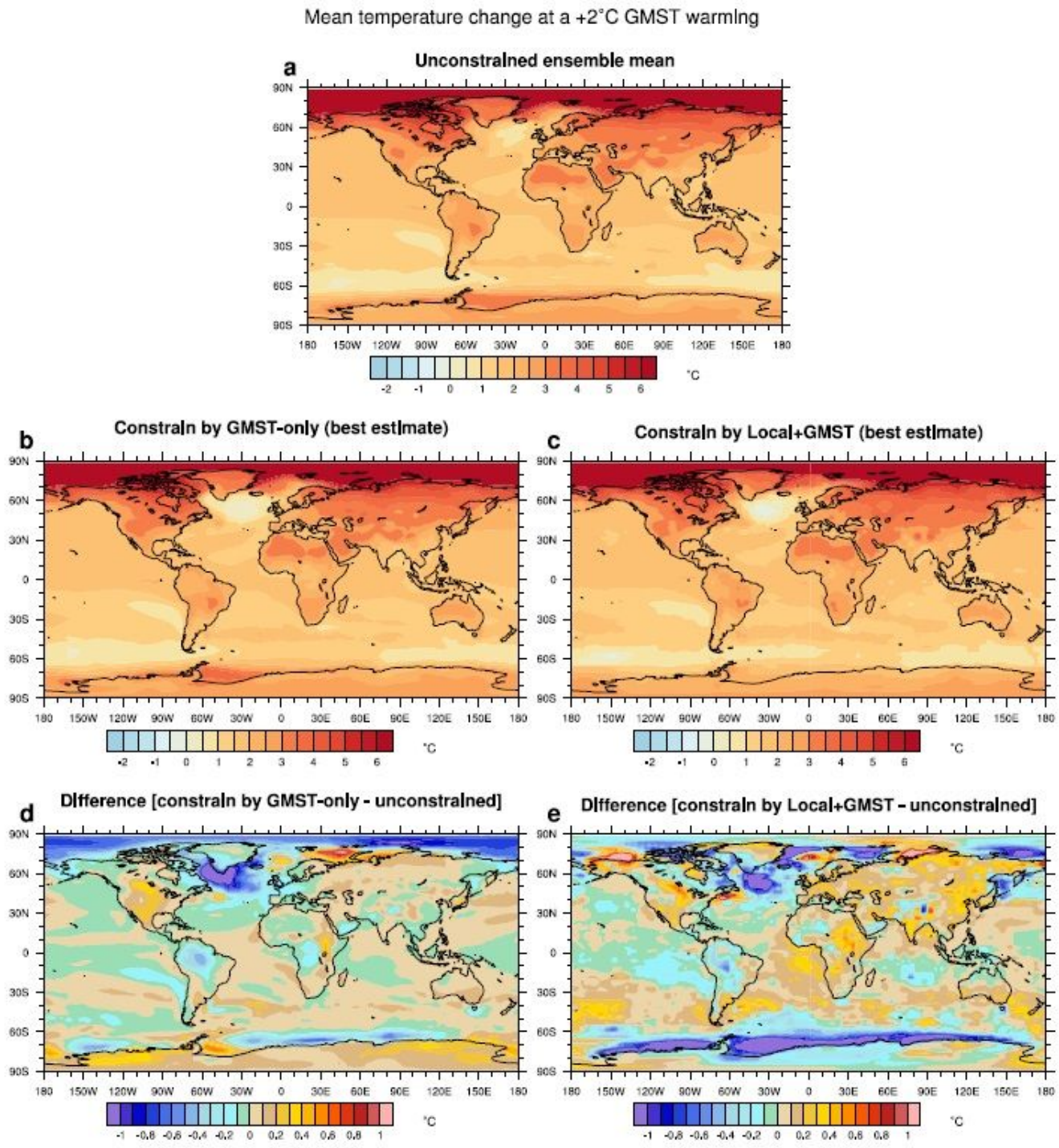

Figure 3

Warming pattern at +2 oC of GMST warming. (a) Ensemble mean of the unconstrained local temperature changes. (b) Best estimate of the constrained local temperature changes in the GMST-only case. (c) Same as (b) but for the Local+GMST case. (d) Difference of local temperature changes between the GMSTonly case (best estimate) and the unconstrained case (ensemble mean). (e) Difference of local temperature changes between the Local+GMST case (best estimate) and the unconstrained case (ensemble mean). All values in (a), (b) and (c) are anomalies with respect to the 1850-1900 period. Note:

The designations employed and the presentation of the material on this map do not imply the expression of any opinion whatsoever on the part of Research Square concerning the legal status of any country, territory, city or area or of its authorities, or concerning the delimitation of its frontiers or boundaries. This map has been provided by the authors.

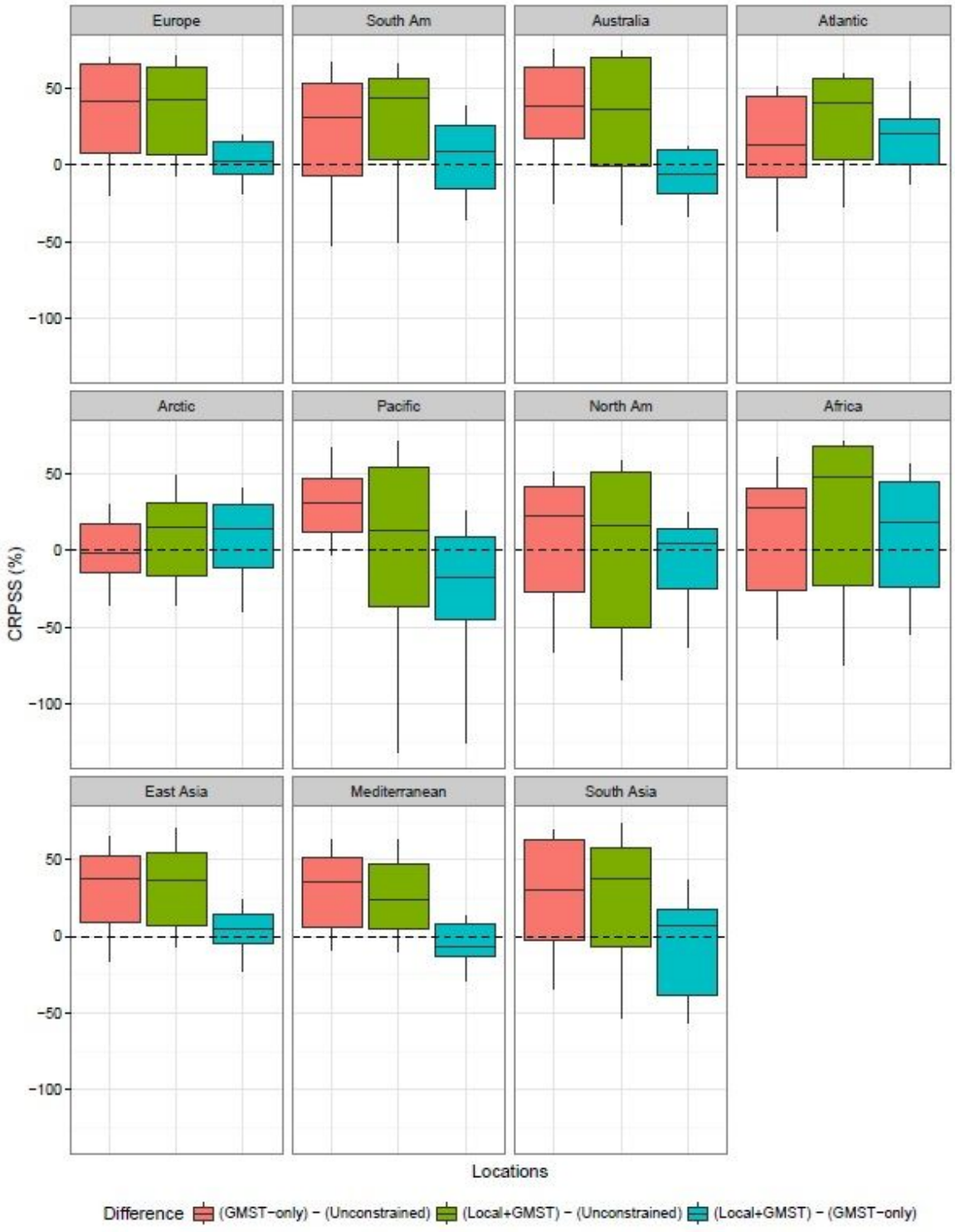

Figure 4

CRPSS for the constrained temperature projections over the 2081-2100 period within the perfect model framework. Red (green) boxplots (one for each location, see blue points in Fig. 1b) indicate the CRPSS distributions in the GMST-only (Local+GMST) case compared to the unconstrained case. Blue boxplots indicate the added value from the local observations and stand for the CRPSS distributions in the Local+GMST case compared to the GMST-only case. The top (bottom) of the box represents the 25th (75th) percentile of the distribution and the upper (lower) whisker represents the 10th (90th) percentile. A CRPSS of 0 (dashed line) indicates the absence of added value of the method.

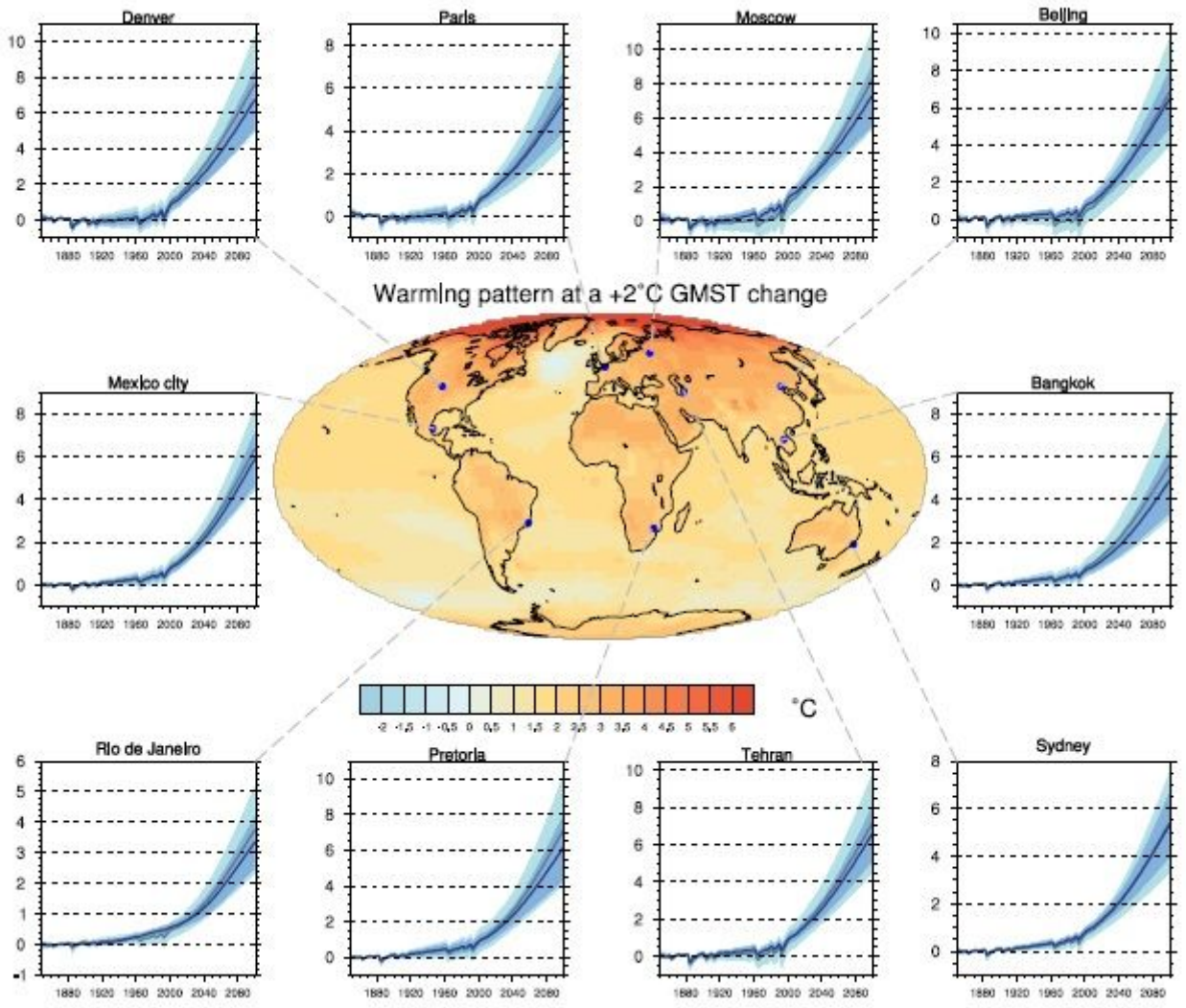

Figure 5

Mean temperature change at a +2 oC GMST warming. Best estimate of the constrained local temperature changes in the Local+GMST case. Similarly to Figure 2b, the constrained and unconstrained temperature ranges are shown for several world capitals cities over the 1850-2100 period. All values are anomalies with respect to the 1850{1900 period. Note: The designations employed and the presentation of the material on this map do not imply the expression of any opinion whatsoever on the part of Research Square concerning the legal status of any country, territory, city or area or of its authorities, or concerning the delimitation of its frontiers or boundaries. This map has been provided by the authors.

Supplementary Files

This is a list of supplementary files associated with this preprint. Click to download.

- SI.pdf
- SI.pdf